Coherence and entanglement in the ground state of a bosonic Josephson junction: From macroscopic Schrödinger cat states to separable Fock states

G. Mazzarella,[1] L. Salasnich,[1,2] A. Parola,[3] and F. Toigo[1]

[1]*Dipartimento di Fisica "Galileo Galilei" and Consorzio Nazionale Interuniversitario per la Scienze Fisiche della Materia (CNISM), Università di Padova, Via Marzolo 8, I-35122 Padova, Italy*

[2]*Istituto Nazionale di Ottica (INO) del Consiglio Nazionale delle Ricerche (CNR), via G. Sansone 1, I-50019 Sesto Fiorentino, Italy*

[3]*Dipartimento di Fisica e Matematica and CNISM,Università dell'Insubria, Via Valleggio 11, I-22100 Como, Italy*

(Received 22 December 2010; published 5 May 2011)

We consider a bosonic Josephson junction made of N ultracold and dilute atoms confined by a quasi-one-dimensional double-well potential within the two-site Bose-Hubbard model framework. The behavior of the system is investigated at zero temperature by varying the interatomic interaction from the strongly attractive regime to the repulsive one. We show that the ground state exhibits a crossover from a macroscopic Schrödinger-cat state to a separable Fock state through an atomic coherent regime. By diagonalizing the Bose-Hubbard Hamiltonian we characterize the emergence of the macroscopic cat states by calculating the Fisher information F, the coherence by means of the visibility α of the interference fringes in the momentum distribution, and the quantum correlations by using the entanglement entropy S. Both Fisher information and visibility are shown to be related to the ground-state energy by employing the Hellmann-Feynman theorem. This result, together with a perturbative calculation of the ground-state energy, allows simple analytical formulas for F and α to be obtained over a range of interactions, in excellent agreement with the exact diagonalization of the Bose-Hubbard Hamiltonian. In the attractive regime the entanglement entropy attains values very close to its upper limit for a specific interaction strength lying in the region where coherence is lost and self-trapping sets in.

DOI: 10.1103/PhysRevA.83.053607 PACS number(s): 03.75.Ss, 03.75.Hh

I. INTRODUCTION

Ultracold and dilute alkali-metal atoms confined in a quasi-one-dimensional (1D) double-well potential [1] are the ideal system to study the Josephson effect [2] and, more generally, the formation of macroscopic coherent states [3–7] and macroscopic Schrödinger-cat states [8–12]. The observed coherent dynamics of the atomic cloud in the double-well potential (bosonic Josephson junction) [1,13] is efficiently described by Josephson equations [3] and their extensions [14–16]. The Josephson equations are valid within the weak interatomic interaction regime, where semiclassical approximations can be performed and the system considered is in a coherent state [17]. When the bosons are repulsively interacting, the crossover from a coherent state (superfluidlike regime) to a separable Fock state (Mott-like regime) takes place by increasing the coupling strength between the atoms [4–7]. This crossover could be detected by measuring the visibility α of the interference fringes in the momentum distribution of the bosonic cloud [4,7]. In the case of attractive coupling, the Josephson equations predict the spontaneous symmetry breaking above a critical strength [3,16], while the two-site Bose-Hubbard model predicts the formation of a macroscopic Schrödinger-cat state [8–12]. Finally, when the attraction between the bosons is sufficiently strong the collapse of the cloud should occur [16,18].

The goal of the present paper is to investigate the coherence and entanglement of the N boson ground state, with particular attention to the formation of macroscopic Schrödinger-cat states, by using as a theoretical tool the two-site Bose-Hubbard (BH) Hamiltonian. Both the experimental implementation of two-mode quantum entangled states and the two-site BH model are the ideal instruments to address the problem of the precision of the difference number and phase measurements [19,20]. In our work, we diagonalize the two-site BH Hamiltonian and evaluate the coherence visibility α, the Fisher information F, and the entanglement entropy S of the ground state. We calculate the Fisher information and the coherence visibility by employing the Hellmann-Feynman theorem (HFT) (see, for example, Ref. [21]) as well. By jointly using this theorem and a perturbative approach for calculating the ground-state energy, we obtain simple analytical formulas for F and α over range of interactions where the perturbative calculation is applicable. This represents one of the main novelties of the present paper. It is quite interesting to compare the results obtained by applying the HFT and those derived from the diagonalization of the BH Hamiltonian. This comparison shows good agreement between the predictions of the two approaches, in particular, for the Fisher information.

The aforementioned quantities, i.e., the Fisher information, the coherence visibility, and the entanglement entropy, are analyzed by widely exploring the atom-atom interaction range, i.e., from strongly attractive to strongly repulsive interactions. This study is, in particular, an analysis of the entanglement entropy, one of the crucial points of our paper. From the above analysis we find that the presence of a macroscopic Schrödinger-cat state [22] in the double well, which can be detected by repeated measurements of the distribution of particles in the two wells [8,9], corresponds to the maximum of the Fisher information F. The maximum of the entanglement entropy S is obtained for attractive interactions close to the onset of coherence loss, which corresponds to the crossover to the self-trapped state. This maximum value is very close to its maximum achievable value, i.e., $\log_2(N+1)$, and greater than that of a macroscopic cat state. For sufficiently strong attractions the coherence visibility α is quite small, but it increases as the interaction strength becomes sufficiently

weak. In addition, we find that by strongly increasing the repulsive interaction, the coherence visibility, the Fisher information F, and the entanglement entropy S go to zero. In this strongly repulsive regime the ground state becomes a separable Fock state with $N/2$ particles in each potential well.

To complete our analysis, we exploit the known fact that the Josephson equations for a bosonic junction can be derived from the two-site Bose-Hubbard Hamiltonian by using the quasiclassical coherent state; this state is characterized by nonvanishing quantum number fluctuations. We compare the N-boson ground-state energy obtained by diagonalizing the BH Hamiltonian with the expectation value of the BH Hamiltonian evaluated with respect to the quasiclassical coherent state. In this way we show the link between the quantum description and the quasiclassical one of the bosonic Josephson junction.

II. THE MODEL HAMILTONIAN

We consider a dilute and ultracold atomic gas made of N identical bosons of mass m confined by a trapping potential $V_{\rm trap}(\mathbf{r})$. This potential can be realized by the superposition of an isotropic harmonic confinement in the the transverse radial plane and a double-well potential $V_{DW}(x)$ in the axial direction x. Then, $V_{\rm trap}(\mathbf{r})$ is given by $V_{\rm trap}(\mathbf{r}) = V_{DW}(x) + m\omega_\perp^2(y^2 + z^2)/2$, where $\omega_\perp$ is the trapping frequency in the radial plane.

We suppose that the system is quasi-one-dimensional due to a strong transverse radial harmonic confinement. In particular, the transverse energy $\hbar\omega_\perp$ is much larger than the characteristic energy of bosons in the axial direction. By assuming that the two wells are symmetric, the microscopic dynamics of our system is described by the effective two-sites BH Hamiltonian [15]:

$$\hat{H} = -J(\hat{a}_L^\dagger \hat{a}_R + \hat{a}_R^\dagger \hat{a}_L) + \frac{U}{2}[\hat{n}_L(\hat{n}_L - 1) + \hat{n}_R(\hat{n}_R - 1)], \tag{1}$$

where $\hat{a}_k, \hat{a}_k^\dagger$ $(k = L, R)$ are bosonic operators satisfying the algebra $[\hat{a}_k, \hat{a}_l^\dagger] = \delta_{kl}$; $\hat{n}_k = \hat{a}_k^\dagger \hat{a}_k$ is the number of particles in the kth well; U is the boson-boson interaction amplitude; and J is the tunnel matrix element between the two wells. Note that the sign of the hopping amplitude can be changed by gauge transformation; in the following we refer to J as a positive quantity. We observe that the total number operator

$$\hat{N} = \hat{n}_L + \hat{n}_R \tag{2}$$

commutes with the Hamiltonian (1), so that the total number of particles is conserved. The macroscopic parameters in the Hamiltonian (1) are explicitly related to the atom-atom coupling constant $g = 4\pi\hbar^2 a_s/m$, a_s being the s-wave scattering length, and to the other microscopic parameters, i.e., the atomic mass m and the frequency $\omega_\perp$ of the harmonic trap (see Ref. [15]). The on-site interaction amplitude U is positive (negative) if a_s is positive (negative), so that it may be changed by Feshbach resonance. The hopping amplitude J is equal to $(\epsilon_1 - \epsilon_0)/2$, where ϵ_0 and ϵ_1 are the ground-state and first-excited-state energies of a single boson in the double well [23].

III. COHERENT, FOCK, AND CAT STATES

At fixed number N of bosons, the ground state of the system depends on the adimensional parameter $\zeta = U/J$. Let us recall what is known in the literature.

(1) In the case of zero interaction ($U = 0$), the ground state of the BH Hamiltonian with a fixed total number N of bosons is the atomic coherent state (ACS)

$$|\mathrm{ACS}\rangle = \frac{1}{\sqrt{\mathrm{N!}}}\left[\frac{1}{\sqrt{2}}(\hat{\mathrm{a}}_\mathrm{L}^\dagger + \hat{\mathrm{a}}_\mathrm{R}^\dagger)\right]^\mathrm{N} |0,0\rangle, \tag{3}$$

where $|0,0\rangle = |0\rangle_L \otimes |0\rangle_R$, that is, the tensor product between the vacuum of the operator $\hat{a}_L$, $|0\rangle_L$ and the vacuum of $\hat{a}_R$, $|0\rangle_R$ [24,25].

(2) In the case of repulsive interaction ($U > 0$) the ground state of the BH Hamiltonian can be found in two very different regimes: the superfluidlike regime and the Mott-like regime [4–7]. The transition from one regime to the other depends on the parameter $\zeta = U/J > 0$. If $\zeta \ll N$, the system is in a quasiclassical superfluid regime characterized by the suppression of phase fluctuations: the ground state is close to $|\mathrm{ACS}\rangle$. If $\zeta \gg N$, the BH Hamiltonian (1) yields the Mott-insulator-like regime where number fluctuations are frozen: the ground state is incoherent [3–7] and close to the separable Fock state,

$$|\mathrm{FOCK}\rangle = \left|\frac{\mathrm{N}}{2}, \frac{\mathrm{N}}{2}\right\rangle. \tag{4}$$

(3) In the case of attractive interaction ($U < 0$) the ground state of the BH Hamiltonian can be close to the atomic coherent state $|\mathrm{ACS}\rangle$ or in an entangled superposition of macroscopic states, i.e., macroscopic Schrödinger-cat states [8–12]. By changing the parameter $\zeta = U/J < 0$, the ground state of the system evolves toward the following macroscopic superposition state:

$$|\mathrm{CAT}\rangle = \frac{1}{\sqrt{2}}(|\mathrm{N},0\rangle + |0,\mathrm{N}\rangle), \tag{5}$$

which is the linear combination of the states with all particles in the left or in the right well. This entangled macroscopic superposition state is also known as the NOON state or "macroscopic cat state." The lower ζ is, the more likely the system is expected to be in the macroscopic Schrödinger-cat state [7–12].

A very interesting issue to address is the study of the coherence and entanglement in a bosonic Josephson junction by varying the ratio U/J from negative to positive values and keeping fixed the number N of atoms. To accomplish this task we solve numerically the following eigenproblem,

$$\hat{H}|E_j\rangle = E_j|E_j\rangle, \tag{6}$$

for a fixed number N of bosons. In this case the Hamiltonian $\hat{H}$ can be represented by a $(N+1)\times(N+1)$ matrix in the Fock basis $|i, N-i\rangle = |i\rangle_L \otimes |N-i\rangle_R$ with $i = 0,\ldots,N$. For each eigenvalue E_j, with $j = 0,1,\ldots,N$, the corresponding eigenstate $|E_j\rangle$ will be of the form

$$|E_j\rangle = \sum_{i=0}^{N} c_i^{(j)} |i, N-i\rangle. \tag{7}$$

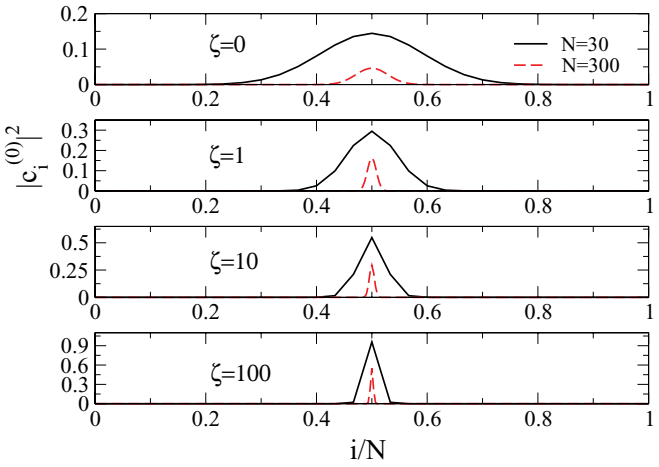

FIG. 1. (Color online) Coefficients $|c_i^{(0)}|^2$ of the repulsive ($U > 0$) ground state $|E_0\rangle$ [see Eq. (7)] of the bosonic junction as a function of i/N. $|c_{i,0}|^2$ are plotted for four values of the adimensional parameter $\zeta = U/J \geqslant 0$. Note that $\sum_{i=0}^{N} |c_i^{(0)}|^2 = 1$ and the total number of coefficients is $N + 1$. The coefficients $|c_i^{(0)}|^2$ and i/N are adimensional quantities.

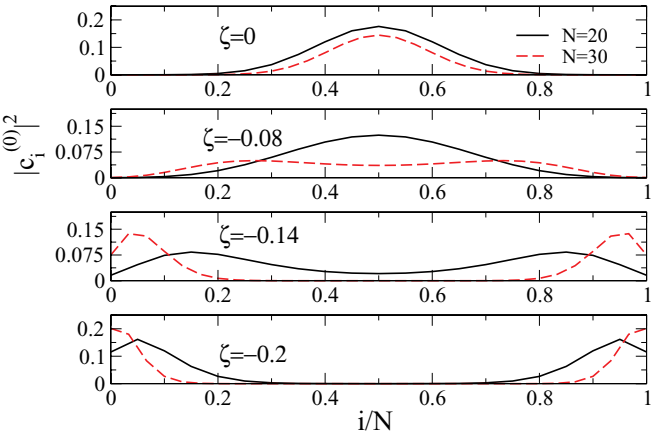

FIG. 2. (Color online) Coefficients $|c_i^{(0)}|^2$ of the attractive ($U < 0$) ground state $|E_0\rangle$ [see Eq. (7)] of the bosonic junction as a function of i/N. $|c_{i,0}|^2$ are plotted for four values of the adimensional parameter $\zeta = U/J \leqslant 0$. The coefficients $|c_i^{(0)}|^2$ and i/N are adimensional quantities.

In Fig. 1 we plot the coefficients $|c_i^{(0)}|^2$ of the repulsive ($U > 0$) ground state $|E_0\rangle$ for different values of the parameter $\zeta = U/J$. In correspondence to each value of ζ, we have studied the ground state for $N = 30$ (solid line) and $N = 300$ (dashed line). Let us focus on the solid line. The figure shows that the width of the peak of $|c_i^{(0)}|^2$ becomes narrower by increasing ζ. Hardening of the localization corresponds to a reduction of the coherence. This is related to the fact that the ground state $|E_0\rangle$ is becoming the "separable Fock state" $|\mathrm{FOCK}\rangle$. The same kind of behavior is observed if the number of particles N is increased. From the plots reported in Fig. 1, we can see that given ζ, the greater N is the stronger the localization.

In Fig. 2 we plot the coefficients $|c_i^{(0)}|^2$ of the attractive ($U < 0$) ground state $|E_0\rangle$ for different values of the parameter $\zeta = U/J$. In correspondence to each value of ζ, we have analyzed the ground state for $N = 20$ (solid line) and $N = 30$ (dashed line). Once the number of bosons N is fixed, we see that by increasing ζ a crossover occurs. There exists a value of ζ, say ζ_{cr} ($\zeta_{cr} \simeq -0.116$ for $N = 20$ and $\zeta_{cr} \simeq -0.076$ for $N = 30$), for which a valley appears in the middle of $|c_i^{(0)}|^2$. This is a signature of the fact that the system is losing coherence and the junction is approaching the self-trapping regime. The above-mentioned crossover takes place from a ground state which has the maximal probability at $i = N/2$ (single peak centered around $i = 0$) for $\zeta = 0$, to a ground state which has the same maximal probability at $i = n$ and $i = N - n$ (two separated peaks symmetric with respect to $i = 0$) with n approaching 0 as ζ decreases. Thus, for a sufficiently small ζ (i.e., $\zeta < 0$ and $|\zeta|$ large) the ground-state $|E_0\rangle$ has the maximal probability to be in the state in which the bosonic population in each well fluctuates around $N/2$. For a sufficiently large ζ, instead, the ground state $|E_0\rangle$ has the maximal probability to be in a "macroscopic cat state": a linear superposition of states with macroscopically different occupations. From the plots shown in Fig. 2, we can see that the larger N is, the larger the attraction for which the crossover to the "macroscopic cat state" occurs.

Finally, we can summarize that Figs. 1 and 2 show the crossover from the macroscopic cat state $|\mathrm{CAT}\rangle$ for $\zeta \ll 0$ to the separable Fock state $|\mathrm{FOCK}\rangle$ for $\zeta \gg 0$, crossing the atomic coherent state $|\mathrm{ACS}\rangle$ at $\zeta = 0$.

It is quite important to note that the ground state $|E_0\rangle$ has definite parity, namely, the distribution of the coefficients $c_i^{(0)}$ is even with respect to $i/N = 1/2$. As consequence, we have that $\langle \hat{n}_L \rangle = N/2 = \langle \hat{n}_R \rangle$.

To conclude this section, we want to stress the role played by the gap, ΔE, between the ground state and the first excited state of the Hamiltonian (1). In fact, when this gap approaches zero, the even and the odd states become quasidegenerate, allowing parity symmetry breaking. Let us focus on the attractive interactions, $U < 0$. In the classical limit, $U \to -\infty$, the ground state is doubly degenerate comprising the two Fock states $|N,0\rangle$ and $|0,N\rangle$. The degeneracy is lifted by quantum fluctuations, and a gap between the even and the odd linear combination of the two Fock states sets in. By standard semiclassical analysis (see Ref. [26]), we can estimate the gap ΔE between the two quasidegenerate ground states in the $|U|N \to \infty$ limit:

$$\Delta E = \frac{|U|\sqrt{N(N+2)}}{\int_0^1 dx\, e^{-Nx^2[2\xi+1+2\ln x]}}\, e^{-N\xi}, \tag{8}$$

where ξ is a positive quantity given by

$$\xi = \ln\left(\frac{|\mathrm{U}|\mathrm{N}}{\mathrm{J}}\right) - 1. \tag{9}$$

This asymptotic expression holds for sufficiently large values of the product UN, as shown in Fig. 3, where ΔE is plotted as a function of N for $U/J = -0.15$. We can see that the diagonalization of the Hamiltonian (1) predicts a gap closing in N according to a law (dashed line) which is well represented by the one given by Eq. (8) (solid line of Fig. 3).

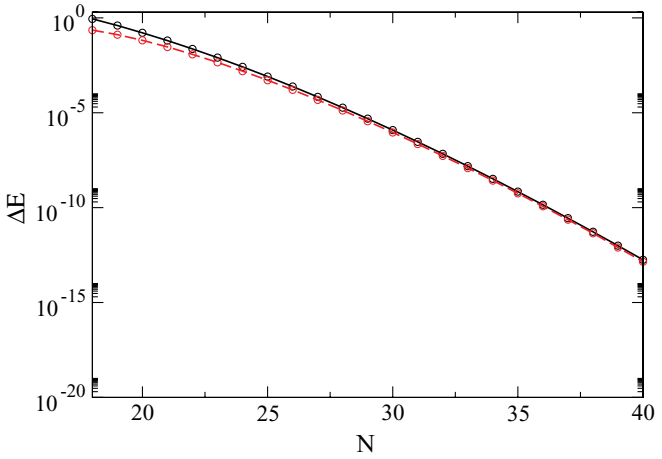

FIG. 3. (Color online) On the vertical axis the energetic gap ΔE at $U/J = -0.15$. On the horizontal axis the number of bosons N. The solid line is obtained with Eq. (8). The circles on the dashed line are the points obtained from the diagonalization of the Hamiltonian (1). Note that the vertical axis is in logarithmic scale. ΔE is in units of J.

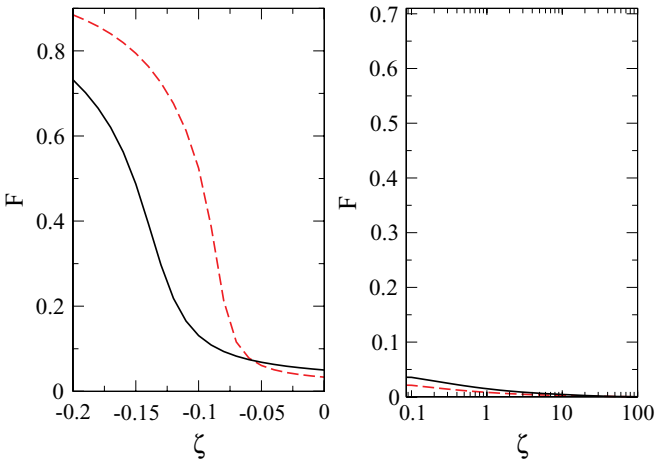

FIG. 4. (Color online) Fisher information F of the ground state $|E_0\rangle$ of the bosonic junction as a function of the parameter $\zeta = U/J$. Left panel: attractive bosons ($U < 0$). Right panel: repulsive bosons ($U > 0$). Solid line: $N = 20$. Dashed line: $N = 30$. Note that the horizontal axis of the right panel is in logarithmic scale. The Fisher information F and ζ are adimensional quantities.

IV. COHERENCE AND ENTANGLEMENT AT ZERO TEMPERATURE

In this section we quantitatively characterize the coherence and the entanglement properties of the ground state by devoting particular attention to the emergence of the macroscopic cat state. Let us start with this last issue. To this end, we recall the definition of the quantum version of the Fisher information $F_{\rm QFI}$ [22,27,28]

$$F_{\rm QFI} = (\Delta \hat{n}_{L,R})^2, \tag{10}$$

where

$$(\Delta \hat{n}_{L,R})^2 = \langle (\hat{n}_L - \hat{n}_R)^2 \rangle - (\langle \hat{n}_L - \hat{n}_R \rangle)^2. \tag{11}$$

It is worth observing that the above definition of the Fisher information, which we use hereafter, holds only for pure states (i.e., only for not mixed states). The expectation values at the right-hand side of Eqs. (10) and (11) are taken with respect to the ground state $|E_0\rangle$ which, having definite parity, satisfies the condition $\langle \hat{n}_L \rangle = \langle \hat{n}_R \rangle$. In terms of the coefficients $c_i^{(0)}$, $F_{\rm QFI}$ is given by

$$F_{\rm QFI} = \sum_{i=0}^{N} [2i - N]^2 |c_i^{(0)}|^2. \tag{12}$$

It is convenient to normalize $F_{\rm QFI}$ at its maximum value N^2 by defining the Fisher information F as

$$F = \frac{F_{\rm QFI}}{N^2}. \tag{13}$$

F gives the width of the distribution $|c_i^{(0)}|^2$ centered at $i/N = 1/2$. As expected, $F = 1$ holds for the macroscopic cat state $|{\rm CAT}\rangle$, and $F = 0$ for the separable Fock state $|FOCK\rangle$.

We have studied F as a function of the parameter $\zeta = U/J$. The results are shown in Fig. 4 for $N = 20$ (solid line) and $N = 30$ (dashed line). The Fisher information F is a monotonic decreasing function of ζ for both attractive and repulsive interactions. On the attractive side (left panel of Fig. 4), there exists a value of ζ, say ζ_F ($\zeta_F \simeq -0.135$ for $N = 20$ and $\simeq -0.08$ for $N = 30$), for which the second derivative of F is zero.

It is quite interesting, now, to observe that by using the HFT theorem (see, for example, Ref. [21]) a relation can be established between the Fisher information F and the partial derivative of the ground-state energy E_0 with respect to U, $\frac{\partial E_0}{\partial U}$. According to the HFT, we have that

$$\frac{\partial E_0}{\partial U} = \langle E_0 | \frac{\partial \hat{H}}{\partial U} | E_0 \rangle. \tag{14}$$

The aforementioned relation is given by the following formula:

$$F = \frac{4}{N^2} \frac{\partial E_0}{\partial U} + \frac{2}{N} - 1. \tag{15}$$

In the limit $U/J \to -\infty$, the hopping operator in Hamiltonian (1) can be treated within perturbation theory. To the zero order, $J = 0$, the energy $E_0^{(0)}$ of the ground state of the on-site interaction operator is $\frac{UN}{2}(N-1)$. This level is twofold degenerate, and the two states corresponding to this energy satisfying $\langle \hat{n}_L \rangle = N/2 = \langle \hat{n}_R \rangle$, i.e., $\frac{1}{\sqrt{2}}(|N,0\rangle + |0,N\rangle)$ and $\frac{1}{\sqrt{2}}(|N,0\rangle - |0,N\rangle)$, have opposite parity.

At the first nonvanishing order the ground-state energy is given by [29]

$$E_0 \simeq E_0^{(0)} + \frac{J^2}{U} \frac{N}{N-1}. \tag{16}$$

By substituting this energy into the expression (15), we obtain

$$F = 1 - \frac{4}{N(N-1)\zeta^2}, \tag{17}$$

which approaches 1 as $\zeta \to -\infty$.

Also in the limit $U/J \to +\infty$, we can treat the hopping operator of the Hamiltonian (1) as a perturbation to the $J = 0$ BH Hamiltonian (1). To the lowest order, the ground-state energy $E_0^{(0)}$ of the on-site interaction operator is equal to $\frac{UN}{2}\left(\frac{N}{2}-1\right)$, which corresponds to the separable Fock state (4). At the first nonvanishing order we get

$$E_0 \simeq E_0^{(0)} - \frac{J^2 N}{U}\left(\frac{N}{2}+1\right). \tag{18}$$

By substituting this energy into the expression (15), we obtain

$$F = \frac{2(N+2)}{N\zeta^2}, \tag{19}$$

which goes to zero as $\zeta \to +\infty$.

In the opposite limit, $U \to 0$, the on-site interaction term can be considered as a perturbation in the Hamiltonian (1). For $U = 0$, the ground-state energy $E_0^{(0)}$ of the hopping operator is equal to $-NJ$, which corresponds to the atomic coherent state (3). To the first order in perturbation theory, we obtain

$$E_0 \simeq E_0^{(0)} + \frac{UN(N-1)}{4}. \tag{20}$$

By substituting this energy into the expression (15), we obtain

$$F = \frac{1}{N}, \tag{21}$$

which tends to 0 when N tends to infinity. In Fig. 5 we show the comparison between the Fisher information F obtained by diagonalizing the Hamiltonian (1) (dashed line) and that obtained by using Eq. (17), attractive bosons, and Eq. (19), repulsive bosons (see the dot-dashed line).

In cold atom physics it is customary to investigate the coherence properties of condensates in terms of their momentum distribution $n(p)$, defined as the Fourier transform of the one-body density matrix $\rho_1(x,x')$ [4,5,7]:

$$n(p) = \int dx dx' \exp[-ip(x-x')]\,\rho_1(x,x'), \tag{22}$$

where

$$\rho_1(x,x') = \langle \hat{\Psi}(x)^\dagger \hat{\Psi}(x') \rangle. \tag{23}$$

Here the operators $\hat{\Psi}(x)$ and $\hat{\Psi}(x)^\dagger$, obeying the standard bosonic commutation rules, annihilate and create, respectively, a boson at the point x; the average $\langle \cdots \rangle$ is the ground-state average. Following Refs. [4,5,7], it is possible to show that the momentum distribution $n(p)$ can be written as

$$n(p) = n_0(p)[1 + \alpha \cos(pd)]. \tag{24}$$

Here $n_0(p)$ is the momentum distribution in the fully incoherent regime [which depends on the shape of the double-well potential $V_{DW}(x)$], and d is the distance between the two minima of $V_{DW}(x)$. α is a real quantity which measures the visibility of the interference fringes. This visibility is given by

$$\alpha = \frac{2\,|\langle \hat{a}_L^\dagger \hat{a}_R \rangle|}{N} \tag{25}$$

and characterizes the degree of coherence between the two wells.

The expectation value of the operator $\hat{a}_L^\dagger \hat{a}_R$ is evaluated in the ground state $|E_0\rangle$ and the visibility α is given by

$$\alpha = \frac{2}{N}\sum_{i=0}^{N} c_i^{(0)} c_{i+1}^{(0)} \sqrt{(i+1)(N-i)}. \tag{26}$$

We have analyzed α as a function of the parameter $\zeta = U/J$ for $N = 20$ (solid line) and $N = 30$ (dashed line). The results of this analysis are reported in Fig. 6. As expected, we see that the coherent state, $\zeta = 0$, has maximum visibility, $\alpha = 1$. On the attractive side (left panel of Fig. 6) there is a value of ζ, say ζ_α, for which the second derivative of α is zero. We have verified that $\zeta_\alpha = \zeta_F$; for a given N such a quantity is close to the aforementioned ζ_{cr}. We observe that both for $N = 20$ and for $N = 30$, the coherence visibility α exhibits a plateau where it is almost independent of the interaction strength and is very close to one. Except for this region, in correspondence to a fixed value of ζ, the greater the value of N the smaller

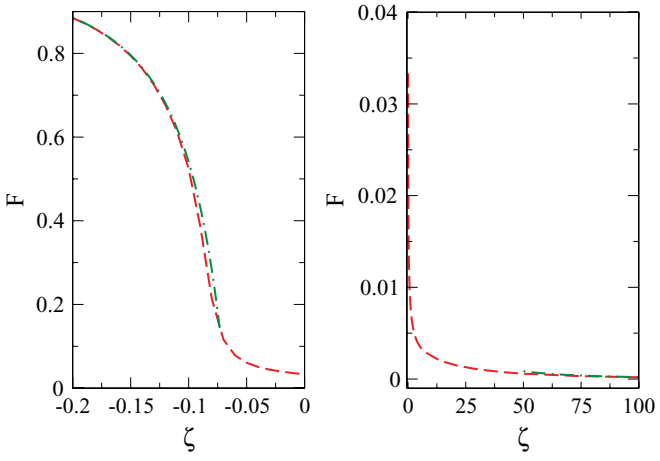

FIG. 5. (Color online) Fisher information F of the ground state $|E_0\rangle$ of the bosonic junction as a function of the parameter $\zeta = U/J$ for $N = 30$. Left panel: attractive bosons ($U < 0$). Right panel: repulsive bosons ($U > 0$). Dashed line: F obtained from the diagonalization of the Hamiltonian (1). Dot-dashed line: F obtained from Eq. (17) ($U < 0$) and Eq. (19) ($U > 0$). The Fisher information F and ζ are adimensional quantities.

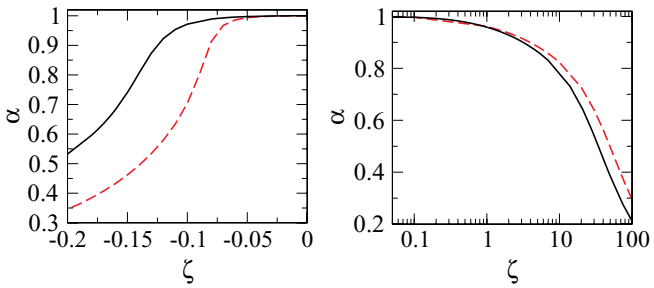

FIG. 6. (Color online) Coherence visibility α of the ground state $|E_0\rangle$ of the bosonic junction as a function of the parameter $\zeta = U/J$. Left panel: attractive bosons ($U < 0$). Right panel: repulsive bosons ($U > 0$). Solid line: $N = 20$. Dashed line: $N = 30$. Note that the horizontal axis of the right panel is in logarithmic scale. The coherence visibility α and ζ are adimensional quantities.

is α. This behavior is reversed for repulsive interactions, as shown in the right panel of Fig. 6, from which we can see that by increasing ζ, α slowly decreases.

The Hellmann-Feynman theorem provides a relation between the coherence visibility α and the derivative of the ground-state energy E_0 with respect to J:

$$\frac{\partial E_0}{\partial J} = \langle E_0| \frac{\partial \hat{H}}{\partial J} |E_0\rangle, \tag{27}$$

leading to

$$\alpha = -\frac{1}{N}\frac{\partial E_0}{\partial J}. \tag{28}$$

By use of the perturbative results previously obtained for the ground-state energy E_0 [see Eqs. (16), (18), and (20)], we can evaluate the coherence visibility (28) in the three regimes $U/J \to -\infty$, $U/J \to +\infty$, and $U \to 0$. In the first case, Eq. (16) gives

$$\alpha = -\frac{2}{(N-1)\zeta}, \tag{29}$$

which, in the limit $\zeta \to -\infty$, tends to 0. For $U/J \to +\infty$, Eq. (18) provides

$$\alpha = \frac{N+2}{\zeta}, \tag{30}$$

which tends to zero when $\zeta \to +\infty$. Finally, at weak coupling ($U \to 0$) the perturbative result (20) gives the limiting value

$$\alpha = 1. \tag{31}$$

In Fig. 7 we show the comparison between the coherence visibility α obtained by diagonalizing the Hamiltonian (1) (dashed line) and that obtained by using Eq. (29) for attractive bosons or Eq. (30) for repulsive bosons (see the dot-dashed line).

At this point we can conclude that the joint application of the HFT and the perturbations theory to calculate the ground-state energy allows very simple analytical formulas to be obtained for the Fisher information F [Eqs. (17) and (19)] and for the coherence visibility α [Eqs. (29) and (30)], at least over a certain range of values of the interaction strength.

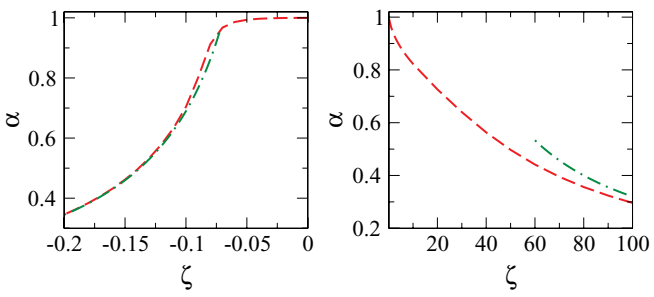

FIG. 7. (Color online) Coherence visibility α of the ground state $|E_0\rangle$ of the bosonic junction as a function of the parameter $\zeta = U/J$ for $N = 30$. Left panel: attractive bosons ($U < 0$). Right panel: repulsive bosons ($U > 0$). Dashed line: α obtained from the diagonalization of the Hamiltonian (1). Dot-dashed line: α from Eq. (29) ($U < 0$) and Eq. (30) ($U > 0$). The coherence visibility α and ζ are adimensional quantities.

We analyze, now, the quantum entanglement pertaining to the ground-state $|E_0\rangle$. When the system is in $|E_0\rangle$, the density matrix $\hat{\rho}$ is

$$\hat{\rho} = |E_0\rangle\langle E_0|. \tag{32}$$

In this case, an excellent measure of the entanglement between the two wells is provided by the entanglement entropy S [30]. This quantity is defined as the von Neumann entropy of the reduced density matrix $\hat{\rho}_L$ defined by

$$\hat{\rho}_L = \mathrm{Tr}_R \hat{\rho}, \tag{33}$$

which is a matrix obtained by partial tracing of the total density matrix (32) over the degrees of freedom of the right well. The entanglement entropy S is given by

$$S = -\mathrm{Tr}\ \hat{\rho}_L \log_2 \hat{\rho}_L = -\sum_{i=0}^{N} \left|c_i^{(0)}\right|^2 \log_2 \left|c_i^{(0)}\right|^2. \tag{34}$$

For a given number of bosons N, the maximum value for S, say $S_{(\max,N)}$, is given by $\log_2(N+1)$. We have studied S as a function of the parameter $\zeta = U/J$ for $N = 20$ (solid line) and $N = 30$ (dashed line). The results of this analysis, which is one of the most crucial studies of this paper, are reported in Fig. 8. We can see that the maximum entanglement is attained for a finite attractive interaction ζ_S. The larger the value of N, the weaker the attraction for which S has a maximum, which is equal to 4.26 when $N = 20$ and 4.72 when $N = 30$. These values are smaller than $S_{(\max,20)} = 4.39$ and $S_{(\max,30)} = 4.95$, respectively, and greater than 1, i.e., the entanglement entropy of a macroscopic cat state (see Table I). The macroscopic cat state is not the maximally entangled state achievable in the bosonic Josephson junction. Moreover, we find that the interactions corresponding to the entanglement entropy maxima are $\zeta_S \simeq -0.13$ for $N = 20$ and $\zeta_S \simeq -0.084$ for $N = 30$. These values are close to the ζ_{cr} values (onset of the coherence loss and the self-trapping regime within the

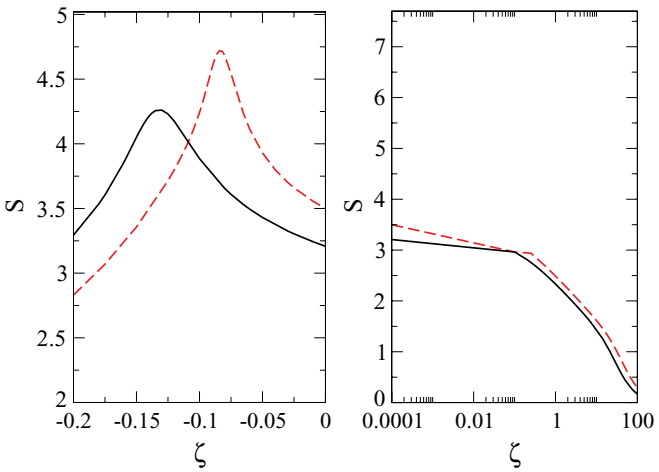

FIG. 8. (Color online) Entanglement entropy S of the ground state $|E_0\rangle$ of the bosonic junction as a function of the parameter $\zeta = U/J$. Left panel: attractive bosons ($U < 0$). Right panel: repulsive bosons ($U > 0$). Solid line: $N = 20$. Dashed line: $N = 30$. Note that the horizontal axis of the right panel is in logarithmic scale. The entanglement entropy S and ζ are adimensional quantities.

TABLE I. The coefficients $c_i^{(0)}$, the zero-temperature Fisher information F, entanglement entropy S, and visibility α for the atomic coherent state (3), the separable Fock state (4), and the macroscopic cat state (5) in the presence of a finite even number N of bosons.

State	$c_i^{(0)}$	F	S	α
$\|\mathrm{ACS}\rangle$	$\left(\frac{1}{2^N}\frac{N!}{i!(N-i)!}\right)^{\frac{1}{2}}$	$\frac{1}{N}$	$\log_2\frac{2^N}{N!}+\frac{1}{2^{N-1}}\sum_{i=2}^{N}\frac{N!}{i!(N-i)!}\log_2 i!$	1
$\|\mathrm{FOCK}\rangle$	$\delta_{i,N/2}$	0	0	0
$\|\mathrm{CAT}\rangle$	$\frac{1}{\sqrt{2}}[\delta_{i,0}+\delta_{i,N}]$	1	1	0

junction dynamics) discussed for the attractive ground-state coefficients (see the discussion regarding Fig. 2).

From the right panel of Fig. 8 we see that for repulsive interactions, S decreases by increasing ζ.

We conclude this section by summarizing, for a finite even number N of bosons and at zero temperature, the expansion coefficients $c_i^{(0)}$, the Fisher information F, the entanglement entropy S, and the visibility α for the atomic coherent state (3), the separable Fock state (4), and the macroscopic cat state (5) (see Table I).

A. Results with two bosons

When $N=2$, it is straightforward to calculate E_j and $|E_j\rangle$. The ground state $|E_0\rangle$ reads

$$|E_0\rangle = A\left(|2,0\rangle + \frac{\zeta+\sqrt{\zeta^2+16}}{2\sqrt{2}}|1,1\rangle + |0,2\rangle\right), \quad (35)$$

where the A is the constant of the normalization, which is

$$A = \frac{2}{\sqrt{16+\zeta^2+\zeta\sqrt{\zeta^2+16}}}. \quad (36)$$

The energy E_0 is

$$E_0 = \frac{U-\sqrt{U^2+16\,J^2}}{2}. \quad (37)$$

The Fisher information (13) calculated with respect to the state (35) is given by the following expression:

$$F = \frac{8}{16+\zeta^2+\zeta\sqrt{\zeta^2+16}}. \quad (38)$$

The coherence visibility (26) for the state (35) is, instead, given by

$$\alpha = \frac{4(\zeta+\sqrt{\zeta^2+16})}{16+\zeta^2+\zeta\sqrt{\zeta^2+16}}. \quad (39)$$

It is possible, also, to evaluate the entanglement entropy (34) when the system is in the state of (37). We have that S can be written as follows:

$$S = -A^2\left(2\log_2\left[\frac{2(\zeta+\sqrt{\zeta^2+16})^2}{(16+\zeta^2+\zeta\sqrt{\zeta^2+16})^2}\right] + \left(\frac{\zeta^2+\zeta\sqrt{\zeta^2+16}}{4}\right)\log_2\left[\frac{(\zeta+\sqrt{\zeta^2+16})^2}{32+2\zeta^2+2\zeta\sqrt{\zeta^2+16}}\right]\right). \quad (40)$$

Concluding, we observe that when $\zeta\to-\infty$ the state (35) tends to

$$|\psi_0\rangle = \frac{1}{\sqrt{2}}(|2,0\rangle+|0,2\rangle). \quad (41)$$

This is the macroscopic superposition state (5) with two bosons. In the limit $\zeta\to-\infty$, the energy (35) tends to $U+\frac{4J^2}{U}$. The Fisher information (38) tends to 1, the coherence visibility (39) to 0, and the entanglement entropy (40) to 1.

When the limit $\zeta\to 0$ is met, the state (35) tends to

$$|\psi_0\rangle = \tfrac{1}{2}(|2,0\rangle+\sqrt{2}|1,1\rangle+|0,2\rangle), \quad (42)$$

which is the atomic coherent state (3) with two bosons. In this case, the energy (37) tends to $-2J$. In the above-mentioned limit, the Fisher information (38) tends to $1/2$, the coherence visibility (39) to 1, and the entanglement entropy (40) to $3/2$, in agreement with the first row of Table I.

Finally, let us analyze the limit $\zeta\to+\infty$. We have that the ground state (35) tends to

$$|\psi_0\rangle = |1,1\rangle, \quad (43)$$

which is the separable Fock state (4) with two bosons. In the previous limit, the Fisher information (38), the coherence visibility (39), and the entanglement entropy (40) tend to 0.

B. Quasiclassical coherent state with number fluctuations

In this section, for the sake of completeness, we compare the N-boson ground state with the quasiclassical coherent state as follows.

The familiar Josephson equations [3,17] of the bosonic Josephson junction can be obtained from the BH Hamiltonian (1) by using the quasiclassical coherent state $|\mathrm{QC}\rangle$. This state is given by the tensor product of the coherent state $|\mathrm{CS}\rangle_\mathrm{L}$, which describes the Bose-Einstein condensate in the left well and the coherent state $|\mathrm{CS}\rangle_\mathrm{R}$, which describes the Bose-Einstein condensate in the right well. The state $|\mathrm{CS}\rangle$ is thus given by

$$|\mathrm{QC}\rangle = |\mathrm{CS}\rangle_\mathrm{L}\otimes|\mathrm{CS}\rangle_\mathrm{R}, \quad (44)$$

where $|\mathrm{CS}\rangle_k$ ($k=\mathrm{L,R}$) is such that [31]

$$|\mathrm{CS}\rangle_k = e^{-|z_k|^2/2}\sum_{n=0}^{\infty}\frac{z_k^n}{\sqrt{n!}}|n\rangle. \quad (45)$$

The complex quantity z_k is the eigenvalue of the annihilator in the kth well, i.e.,

$$\hat{a}_k|\mathrm{CS}\rangle_k = z_k\,|\mathrm{CS}\rangle_k. \tag{46}$$

The absolute values of the two z_k are related to the average occupancy of the two wells:

$$N_k \equiv \langle \mathrm{QC}|\hat{n}_k|\mathrm{QC}\rangle = |z_k|^2. \tag{47}$$

so z_k are conveniently parameterized as $z_k = \sqrt{N_k}\exp(i\theta_k)$, where θ_k are phase variables. The quasiclassical coherent state $|\mathrm{QC}\rangle$ does not have a fixed number of particles and consequently allows for nonvanishing quantum fluctuations of the total number of bosons. The average boson number in the state $|\mathrm{QC}\rangle$ is simply given by $N = N_L + N_R = |z_L|^2 + |z_R|^2$.

The expectation value E of the BH Hamiltonian (1) evaluated with respect to the state (44) is

$$E = \langle \mathrm{QC}|\hat{H}|\mathrm{QC}\rangle = -N\,J\sqrt{1-z^2}\cos\phi + \frac{N^2\,U}{4}(1+z^2), \tag{48}$$

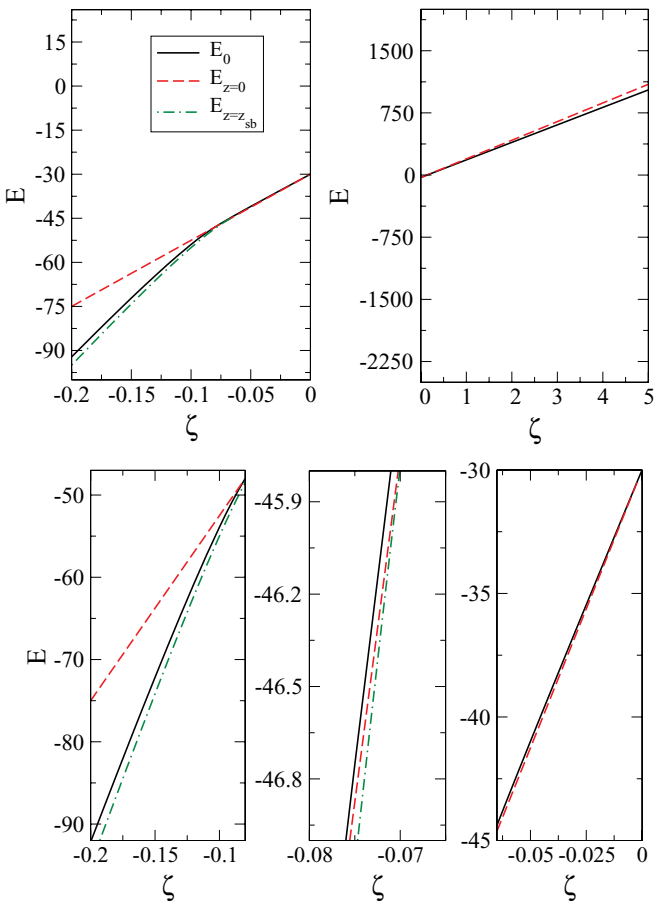

FIG. 9. (Color online) On the vertical axis, the energy of the ground state $|E_0\rangle$, E_0 (solid line), the energy (48) calculated for $z = 0$, $E_{z=0}$ (dashed line), and the energy (48) calculated for $z = z_{sb}$, $E_{z=z_{sb}}$ (dot-dashed line). On the horizontal axis the parameter $\zeta = U/J$. Left part of the upper panel: attractive bosons ($U < 0$). Right part of the upper panel: repulsive bosons ($U > 0$). Lower panels: three insets for attractive bosons. We have set $N = 30$. E is in units of J, and ζ is an adimensional quantity.

where $z = (N_L - N_R)/N$ and $\phi = \theta_R - \theta_L$. In formula (48) we recognize the total energy of a nonrigid pendulum, which represents the mechanic analog of a bosonic Josephson junction [3,17]. In fact, the state $|\mathrm{QC}\rangle$ is expected to be close to the ground state $|E_0\rangle$ in the weak-coupling regime [17]. It is straightforward to show that the minima of the energy (48) are obtained with $\phi = 0$ and

$$z = z_{sb} = \pm\sqrt{1 - \frac{4}{\zeta^2 N^2}} \quad \text{if} \quad \zeta < -\frac{2}{N}$$
$$z = 0 \quad \text{if} \quad \zeta > -\frac{2}{N}. \tag{49}$$

Note that $\zeta = -2/N$ signals the onset of the self-trapping regime within an attractive 1D bosonic Josephson junction [16]. The energy (48) calculated for $z = 0$, say $E_{z=0}$, and for $z = z_{sb}$, say $E_{z=z_{sb}}$, becomes

$$E_{z=0} = N\left(\frac{N\,U}{4} - 1\right) \tag{50}$$

$$E_{z=z_{sb}} = \frac{J^2}{U} + \frac{N^2\,U}{2}. \tag{51}$$

It is interesting to compare the energy E of the quasiclassical state $|\mathrm{QC}\rangle$ with the energy E_0 of the state $|E_0\rangle$, that is, the ground state of the BH Hamiltonian with a fixed number N of bosons (see also Ref. [32]). From the upper right panel of Fig. 9, obtained with $N = 30$, we see that for repulsive bosons, E_0 (solid line) is smaller than $E_{z=0}$ (dashed line). For attractive bosons, the situation is much more complex. Let us focus on the lower panels of Fig. 9. We can see that there are three different regions. In the first one [left panel: $\zeta < -2/N - \Delta$ ($\Delta > 0$)] we have that $E_{z=z_{sb}} < E_0 < E_{z=0}$; in the second region (middle panel: $-2/N - \Delta < \zeta < -2/N$) we have that $E_{z=z_{sb}} < E_{z=0} < E_0$; in the third region (right panel: $\zeta > -2/N$) we have that $E_{z=0} < E_0$. Note that the greater is N the smaller is Δ.

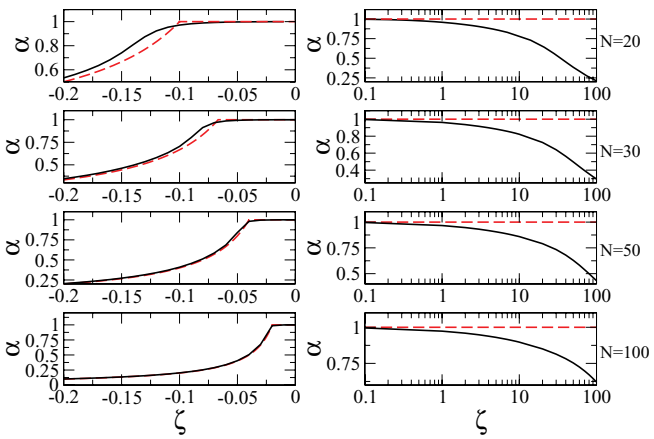

FIG. 10. (Color online) Coherence visibility α of the bosonic junction as a function of the dimensionless parameter $\zeta = U/J$. Left panel: attractive bosons ($U < 0$). Right panel: repulsive bosons ($U > 0$). Solid line: results from Eq. (26). Dashed line: results from Eq. (52). Note that the horizontal axis of the right panel is in logarithmic scale. The coherence visibility α and ζ are adimensional quantities.

The coherence visibility (25) calculated with respect to the state $|\mathrm{QC}\rangle$ reads

$$\alpha = \sqrt{1 - z^2}, \tag{52}$$

with z given by Eqs. (49). In Fig. 10 we report the comparisons between the coherence visibility calculated by using the ground state $|E_0\rangle$ of the BH Hamiltonian (1) and that calculated by using Eq. (52). Figure 10 clearly shows that the coherence visibility α of the quasiclassical coherent state $|\mathrm{QC}\rangle$ is strictly equal to one only for a non-negative interaction strength. Moreover, from the left panels (attractive bosons) of Fig. 10, we can see that the greater the number of particles in the system, the better the agreement between the predictions derived from the two approaches.

The Fisher information F, Eqs. (12) and (13), calculated with respect to the state $|\mathrm{QC}\rangle$, is simply given by

$$F = \frac{1}{N}. \tag{53}$$

This is the same result that one obtains when the system is in the atomic coherent state (3), i.e., the exact eigenstate for $U = 0$.

V. CONCLUSIONS

We have investigated an atomic Josephson junction in the presence of a finite number of interacting ultracold bosons confined in a quasi-one-dimensional geometry. By using the two-site Bose-Hubbard Hamiltonian toolbox, we have carried out zero-temperature analysis by finding the ground state of the system. We have characterized the presence of macroscopic Schrödinger-cat states, the coherence properties, and quantum correlations by calculating the Fisher information, the visibility of the interference fringes in the momentum distribution, and the entanglement entropy as functions of the boson-boson interaction strength. The joint application of the Hellmann-Feynman theorem and of the perturbative approach to evaluate the ground-state energy allows analytical formulas to be obtained, within the interactions range in which the perturbative theory is applicable, both for the Fisher information and for the coherence visibility. The Fisher information and the coherence visibility predicted by these formulas are in good agreement with those evaluated by diagonalizing the two-site Bose-Hubbard Hamiltonian. In the attractive regime we have found that the presence of macroscopic Schrödinger-cat states corresponds to a maximum of the Fisher information, while the entanglement entropy has a maximum when the system begins to lose coherence and to exhibit self-trapped dynamics. The maximal entanglement entropy is larger than that of a macroscopic cat state and, in fact, is very close to its theoretical upper limit.

ACKNOWLEDGMENTS

G.M. thanks Alessio Serafini and S. M. Giampaolo for useful discussions.

[1] O. Morsch and M. Oberthaler, Rev. Mod. Phys. **78**, 179 (2006).
[2] A. Barone and G. Paternò, *Physics and Applications of the Josephson Effect* (Wiley, New York, 1982).
[3] S. Raghavan, A. Smerzi, S. Fantoni, and S. R. Shenoy, Phys. Rev. A **59**, 620 (1999).
[4] L. Pitaevskii and S. Stringari, Phys. Rev. Lett. **83**, 4237 (1999); **87**, 180402 (2001).
[5] J. R. Anglin, P. Drummond, and A. Smerzi, Phys. Rev. A **64**, 063605 (2001).
[6] K. W. Mahmud, H. Perry, and W. P. Reinhardt, J. Phys. B **36**, L265 (2003); Phys. Rev. A **71**, 023615 (2005).
[7] G. Ferrini, A. Minguzzi, and F. W. J. Hekking, Phys. Rev. A **78**, 023606(R) (2008).
[8] J. I. Cirac, M. Lewenstein, K. Molmer, and P. Zoller, Phys. Rev. A **57**, 1208 (1998).
[9] D. A. R. Dalvit, J. Dziarmaga, and W. H. Zurek, Phys. Rev. A **62**, 013607 (2000).
[10] Y. P. Huang and M. G. Moore, Phys. Rev. A **73**, 023606 (2006).
[11] L. D. Carr, D. R. Dounas-Frazer, and M. A. Garcia-March, Europhys. Lett. **90**, 10005 (2010).
[12] D. W. Hallwood, T. Ernst, and J. Brand, Phys. Rev. A **82**, 063623 (2010).
[13] F. S. Cataliotti *et al.*, Science **293**, 843 (2001); Y. Shin, M. Saba, T. A. Pasquini, W. Ketterle, D. E. Pritchard, and A. E. Leanhardt, Phys. Rev. Lett. **92**, 050405 (2004); M. Albiez, R. Gati, J. Folling, S. Hunsmann, M. Cristiani, and M. K. Oberthaler, *ibid*. **95**, 010402 (2005); S. Levy *et al.*, Nature (London) **499**, 579 (2007).
[14] G. Mazzarella, M. Moratti, L. Salasnich, M. Salerno, and F. Toigo, J. Phys. B **42**, 125301 (2009).
[15] G. Mazzarella, M. Moratti, L. Salasnich, and F. Toigo, J. Phys. B **43**, 065303 (2010).
[16] G. Mazzarella and L. Salasnich, Phys. Rev. A **82**, 033611 (2010).
[17] A. J. Leggett, *Quantum Fluids* (Oxford University Press, Oxford, 2006).
[18] L. Salasnich, B. A. Malomed, and F. Toigo, Phys. Rev. A **81**, 045603 (2010).
[19] J. Estève, C. Gross, A. Weller, S. Giovanazzi, and M. K. Oberthaler, Nature **455**, 1216 (2010); C. Gross, T. Zibold, E. Nicklas, J. Estève, and M. K. Oberthaler, *ibid*. **464**, 1165 (2010).
[20] C. Bodet, J. Estève, M. K. Oberthaler, and T. Gasenzer, Phys. Rev. A **81**, 063605 (2010).
[21] C. Cohen-Tannoudji, B. Diu, and F. Laloe, *Quantum Mechanics* (J. Wiley, New York, 1977), Vol. 2.
[22] L. Pezzè and A. Smerzi, Phys. Rev. Lett. **102**, 100401 (2009).
[23] L. Salasnich, G. Mazzarella, M. Salerno, and F. Toigo, Phys. Rev. A **81**, 023614 (2010).
[24] F. T. Arecchi, E. Courtens, R. Gilmore, and H. Thomas, Phys. Rev. A **6**, 2211 (1972); G. J. Milburn, J. Corney, E. M. Wright, and D. F. Walls, *ibid*. **55**, 4318 (1997).
[25] B. Julia-Diaz, D. Dagnino, M. Lewenstein, J. Martorell, and A. Polls, Phys. Rev. A **81**, 023615 (2010).
[26] L. Landau and L. Lifshitz, *Course in Theoretical Physics*, *Quantum Mechanics: Non-Relativistic Theory*, (Pergamon, New York, 1959), Vol. 3.

[27] W. K. Wootters, Phys. Rev. D **23**, 357 (1981); C. W. Helstrom, *Quantum Detection and Estimation Theory* (Academic Press, New York, 1976), Chap. VIII; A. S. Holevo, *Probalistic and Statistical Aspect of Quantum Theory* (North-Holland, Amsterdam, 1982); S. L. Braunstein and C. M. Caves, Phys. Rev. Lett. **72**, 3439 (1994).

[28] B. Gertjerenken, S. Arlinghaus, N. Teichmann, and C. Weiss, Phys. Rev. A **82**, 023620 (2010).

[29] We note that for $N = 2$, the second-order perturbation theory lifts the degeneracy between the even and the odd parity states, which are shifted by $\pm 2J^2/U$ with respect to the classical value [see Eq. (37)], leading to a splitting $\Delta E = \frac{4J^2}{|U|}$. For $N > 2$ second-order perturbation theory does not remove the ground-state degeneracy.

[30] C. H. Bennett, H. J. Bernstein, S. Popescu, and B. Schumacher, Phys. Rev. A **53**, 2046 (1996); S. Hill and W. K. Wootters, Phys. Rev. Lett. **78**, 5022 (1997); L. Amico, R. Fazio, A. Osterloh, and V. Vedral, Rev. Mod. Phys. **80**, 517 (2008); J. Eisert, M. Cramer, and M. B. Plenio, ibid. **82**, 277 (2010).

[31] R. J. Glauber, Phys. Rev. **131**, 2766 (1963).

[32] P. Buonsante, P. Kevrekidis, V. Penna, and A. Vezzani, J. Phys. B **39**, S77 (2006)